American Mineralogist, Volume 80, pages 732–743, 1995

Geochemical alteration of pyrochlore group minerals: Pyrochlore subgroup

Gregory R. Lumpkin
Advanced Materials Program, Australian Nuclear Science and Technology Organization, Menai 2234, New South Wales, Australia
Rodney C. Ewing
Department of Earth and Planetary Sciences, University of New Mexico, Albuquerque, New Mexico 87131, U.S.A.

Abstract

Primary alteration of uranpyrochlore from granitic pegmatites is characterized by the substitutions $^{A}\square^{Y}\square \rightarrow {}^{A}Ca^{Y}O$, $^{A}Na^{Y}F \rightarrow {}^{A}Ca^{Y}O$, and $^{A}Na^{Y}OH \rightarrow {}^{A}Ca^{Y}O$. Alteration occurred at ~450–650 °C and 2–4 kbar with fluid-phase compositions characterized by relatively low a_{Na^+}, high $a_{Ca^{2+}}$, and high pH. In contrast, primary alteration of pyrochlore from nepheline syenites and carbonatites follows a different trend represented by the substitutions $^{A}Na^{Y}F \rightarrow {}^{A}\square^{Y}\square$ and $^{A}Ca^{Y}O \rightarrow {}^{A}\square^{Y}\square$. In carbonatites, primary alteration of pyrochlore probably took place during and after replacement of diopside + forsterite + calcite by tremolite + dolomite ± ankerite at ~300–550 °C and 0–2 kbar under conditions of relatively low a_{HF}, low a_{Na^+}, low $a_{Ca^{2+}}$, low pH, and elevated activities of Fe and Sr. Microscopic observations suggest that some altered pyrochlores are transitional between primary and secondary alteration. Alteration paths for these specimens scatter around the trend $^{A}Na^{Y}F \rightarrow {}^{A}\square^{Y}\square$. Alteration probably occurred at 200–350 °C in the presence of a fluid phase similar in composition to the fluid present during primary alteration but with elevated activities of Ba and REEs. Mineral reactions in the system Na-Ca-Fe-Nb-O-H indicate that replacement of pyrochlore by fersmite and columbite occurred at similar conditions with fluid conpositions having relatively low a_{Na^+}, moderate $a_{Ca^{2+}}$, and moderate to high $a_{Fe^{2+}}$. Secondary alteration (<150 °C) is characterized by the substitutions $^{A}Na^{Y}F \rightarrow {}^{A}\square^{Y}\square$, $^{A}Ca^{Y}O \rightarrow {}^{A}\square^{Y}\square$, and $^{A}Ca^{X}O \rightarrow {}^{A}\square^{X}\square$ together with moderate to extreme hydration (10–15 wt% H_2O or 2–3 molecules per formula unit). Minor variations in the amounts of Mg, Al, K, Mn, Fe, Sr, Ba, and REEs are commonly observed as a result of secondary alteration. Major cation exchange for K, Sr, and Ba is a feature of samples from laterite horizons overlying carbonatites. In most cases U, Th, and B-site cations remain relatively constant. Radiogenic Pb is typically lost via long-term diffusion, but in some grains of uranpyrochlore 25–90% of the Pb is lost as a result of alteration.

Introduction

The pyrochlore group consists of a chemically diverse suite of minerals having the general formula $A_{2-m}B_2X_{6-w}Y_{1-n}\cdot pH_2O$, where A = Na, Ca, Mn, Fe^{2+}, Sr, Sb, Cs, Ba, rare earth elements (REEs = Sc, Y, lanthanides), Pb, Bi, Th, and U; B = Nb, Ta, Ti, Al, Fe^{3+}, Zr, Sn, and W; X = O, OH; and Y = O, OH, and F. The structure type is cubic (space group $Fd3m$, $Z = 8$), has a unit cell dimension of approximately 10.3–10.6 Å, and tolerates vacancies at the A, X, and Y sites ($m = 0$–1.7, $w = 0$–0.7, $n = 0$–1). Defect pyrochlore may be stabilized by the incorporation of H_2O molecules ($p = 0$–2) and OH groups, with total H_2O contents of 10–15 wt% (Lumpkin, 1989). Hogarth (1977) defined three major subgroups of the pyrochlore group on the basis of the major B-site cations: microlite (Nb + Ta > 2Ti, Ta ≥ Nb), pyrochlore (Nb + Ta > 2Ti, Nb > Ta), and betafite (2Ti ≥ Nb + Ta). Individual species in each subgroup are defined by the A-site cation population (see Hogarth, 1977, Table 1).

Microlite is mainly restricted to moderately to highly fractionated rare-element granitic pegmatites; betafite is found in geochemically more primitive granitic pegmatites and in some carbonatites (Černý and Ercit, 1989). Members of the pyrochlore subgroup predominantly occur in three major host rock categories: carbonatites, nepheline syenites, and granitic pegmatites. As a result, the general chemistry of the pyrochlore subgroup is extremely diverse in relation to the microlite and betafite subgroups (e.g., Hogarth, 1961; Perrault, 1968; Krivokoneva and Sidorenko, 1971; Petruk and Owens, 1975). Because of the variety of host rocks encountered as well as the complex compositions of members of the pyrochlore subgroup, chemical effects of alteration are expected to be complicated (Lumpkin and Ewing, 1985).

Geochemical alteration of pyrochlore in carbonatites to a hydrated, defect pyrochlore enriched in Ba, Sr, or K

0003–004X/95/0708–0732$02.00

TABLE 1. Localities, sources, host rocks, and associated minerals for 18 pyrochlore samples

No.	Locality and host rock type	Alteration pattern and mineral association	I/I_0	Source
084	Brevik, Norway; nepheline syenite	3 mm octahedron with secondary alteration along fractures, Pl + Ap + Zrn	0.0	USNM B20541
086	Lueshe, Lake Kivu, Zaire; carbonatite	3 mm heavily fractured gray crystal from laterite, complete secondary alteration	0.8–0.9	USNM 117122
090	Hybla, Ontario, Canada; granitic pegmatite	>1 cm mass, transitional alteration, Qtz + Cal + Pl	0.0	USNM 94802
177	Brevik, Norway; nepheline syenite	0.2–1 mm crystals with transitional alteration overprinted by secondary alteration along fractures, Kfs + Am + Bt ± Fl	—	AMNH C67239
181	Stoken, Langesundfiord, Norway; nepheline syenite	0.1–1 mm crystals with primary alteration overprinted by transitional alteration, Kfs + Pyx + Ap	—	AMNH 24334
187	Alnö, Sweden; carbonatite	1–2 mm crystals with primary alteration overprinted by transitional alteration, Cal + Ap + Phl + Ol ± Srp	0.2	AMNH 24310
191	Gastineau River, Ontario, Canada; carbonatite	0.2–2 mm crystals, heavily fractured, smaller grains exhibit complete secondary alteration, Cal + Bt + Ap	0.0	AMNH 39924
197	Panda Hill, Mbeya, Tanzania; carbonatite	3 mm heavily fractured crystal from laterite, secondary alteration plus unaltered relicts	0.3–0.4	AMNH 25430
214	Woodcox mine, Hybla, Ontario; granitic pegmatite	>1 cm mass with transitional alteration and fracture controlled secondary alteration, Kfs + Pl + Qtz	0.0	HU 1024503
216	MacDonald mine, Hybla, Ontario; granitic pegmatite	>2 cm mass with primary alteration overprinted by fracture controlled secondary alteration, Cal + Zrn + Qtz	0.0	HU 118064
289	MacDonald mine, Hybla, Ontario; granitic pegmatite	0.2–2 cm crystals with transitional alteration along crystal margins, Cal + Qtz ± Zrn	0.0	UNM
290	Panda Hill, Mbeya, Tanzania; carbonatite	5 mm single crystal, zoned, unaltered, Cal + Am + Bt + Ap + Mag ± Zrn	0.8–1.0	USNM 120178
294	Leushe, Lake Kivu, Zaire; carbonatite	4 mm greenish-gray single crystal from laterite, heavily fractured, complete secondary alteration	0.8–0.9	USNM 117122
298	Fredricksvarn, Norway; nepheline syenite	0.1–1 mm crystals with secondary alteration along crystal rims, Kfs + Bt + Am + Ap ± Zrn ± Ttn ± Mag ± Ilm	—	USNM R5033
299A	Lueshe, Lake Kivu, Zaire; carbonatite	5 mm single crystal, unaltered, Cal + Pyx + Ap ± Pl	0.5–0.8	USNM 114776
299B	Lueshe, Lake Kive, Zaire; carbonatite	4 mm greenish-gray single crystal from laterite, heavily fractured, complete secondary alteration	0.9–1.0	USNM 114776
325	Jacupiranga, Sao Paulo, Brazil; carbonatite	1–2 mm crystals with primary alteration of crystal rims, baddeleyite inclusions, Cal + Ap + Mag + Ol ± Srp ± Phl ± Ilm	0.2–0.3	UNM
1C24	Araxá, Minas Gerais, Brazil; carbonatite	0.1–1 mm tan crystals from laterite, microfractured, turbid secondary alteration, plus relicts of unaltered pyrochlore phase	—	A.N. Mariano

Note: I/I_0 determined by XRD ranges from 0.0 for completely metamict samples to 1.0 for highly crystalline samples. Am = amphibole; Ap = apatite; Bt = biotite; Cal = calcite; Fl = fluorite; Ilm = ilmenite; Kfs = potassium feldspar; Mag = magnetite; Ol = olivine; Phl = phlogopite; Pl = plagioclase; Pyx = pyroxene; Qtz = quartz; Srp = serpentine; Ttn = titanite; Zrn = zircon.

has been documented in several prior studies (e.g., Jäger et al., 1959; van der Veen, 1963; Harris, 1965; Van Wambeke, 1971, 1978). The general consensus is that alteration occurred under low-temperature hydrothermal conditions or as a direct result of weathering of the host rock. A range of alteration products of pyrochlore have also been noted in the literature, including columbite, fersmite, lueshite, bastnaesite, and several iron titanium oxides (James and McKie, 1958; van der Veen, 1960, 1963; Skorobogatova, 1963; Van Wambeke, 1970; Heinrich, 1980). Chemical reactions involving these minerals and pyrochlore indicate that Fe, Ca, Na, and REEs may be important constituents of the fluid phase during alteration, and, in specific cases, the B-site cations Nb, Ti, and Zr may have been mobile (see Gieré, 1990, for recent evidence on the mobility of Ti, Zr, and REEs in hydrothermal fluids).

Apart from the available information in the literature on pyrochlores from carbonatites and their overlying laterites, the chemical effects of alteration in members of the pyrochlore subgroup from granitic pegmatites and nepheline syenites are virtually unknown. The goal of this investigation is to establish a general chemical framework for the interaction of minerals of the pyrochlore subgroup with high-temperature fluids that evolve during host rock emplacement and with later, lower temperature hydrothermal fluids and ground waters. Furthermore, the results of this work provide additional information on the long-term performance of crystalline phases with the pyrochlore structure in ceramic nuclear waste forms, including Synroc, tailored ceramics, and lanthanum zirconium oxide (e.g., Ringwood et al., 1988; Harker, 1988; Hayakawa and Kamizono, 1993).

SAMPLE DESCRIPTION

A detailed description of each sample is given in Table 1 using the previously adopted criteria for recognition of alteration (Lumpkin and Ewing, 1992; see also Van Wambeke, 1970; Ewing, 1975). In general, primary alteration is characterized by large-scale intracrystalline diffusion with limited fracture control (e.g., samples 181, 187, 216, and 325; see Fig. 1a). In carbonatites, primary

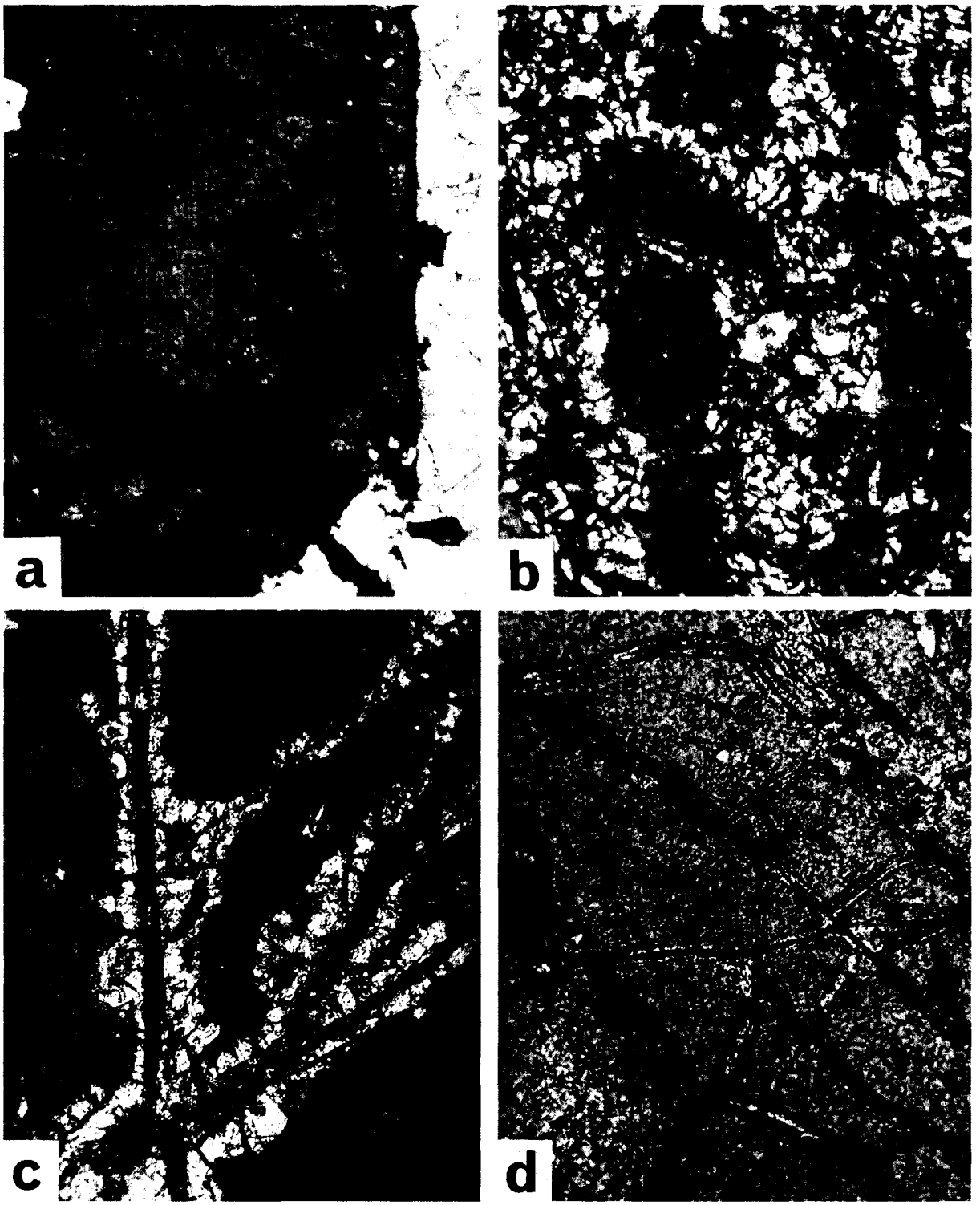

Fig. 1. Optical micrographs showing alteration effects in minerals of the pyrochlore subgroup. (**a**) Pale green primary alteration surrounding unaltered yellow-orange core, sample 187, Alnö carbonatite, field of view 1.0 × 0.8 mm. (**b**) Colorless transitional alteration surrounding unaltered yellow-brown areas, sample 289, MacDonald pegmatite, field of view 1.0 × 0.8 mm. (**c**) Colorless secondary alteration localized along microfractures, sample 214, Woodcox pegmatite, field of view 0.5 × 0.4 mm. (**d**) Secondary alteration localized along microfractures, sample 084, nepheline syenite, Norway, field of view 1.0 × 0.8 mm.

alteration of pyrochlore may be associated with the replacement of the diopside + olivine + calcite assemblage by tremolite + dolomite. In contrast, secondary alteration is strongly fracture controlled (e.g., samples 084 and 214; see Fig. 1c and 1d) and is often associated with the alteration of feldspars and micas to clay minerals, chlorite, and iron oxides. Some heavily fractured crystals from laterite zones overlying carbonatites may be completely altered, having a turbid appearance in thin section (samples 086, 294, 299B, 197, and 1C24).

On the basis of established textural criteria for recognition of alteration, several specimens were found to exhibit a style of alteration between the extremes defined as primary and secondary (Table 1). Defined as transitional alteration, this pattern is characterized by a combination of intracrystalline diffusion and fracture control (e.g., samples 090, 177, 181, 187, and 289; see Fig. 1b). Transitional alteration of pyrochlore from carbonatites may be associated with the alteration of olivine, pyroxene, amphibole, and mica to serpentine, sodium amphibole, talc, and chlorite.

Niobium oxide mineral reactions

Idealized phase relations between pyrochlore and associated niobium oxide minerals can be depicted in the system Na-Ca-Fe-Nb-O-H by replacing Mn and Ta in the reactions listed in Table 2 of Lumpkin and Ewing (1992) with Fe and Nb, respectively. This system is represented in carbonatites by the common association of pyrochlore, ferrocolumbite, fersmite, and lueshite or natroniobite (e.g., James and McKie, 1958; van der Veen, 1960, 1963; Heinrich, 1980). In Figure 2 we have constructed schematic phase relations based on the idealized compositions of pyrochlore ($NaCaNb_2O_{6.5}$), ferrocolumbite ($FeNb_2O_6$), fersmite ($CaNb_2O_6$), and lueshite ($NaNbO_3$) together with the hypothetical phases Nb_2O_5, $Na_2Nb_4O_{11}$, $CaNb_4O_{11}$, and $Ca_2Nb_2O_7$. Mineral phases known to exist in this system are shown by circles, whereas the observed replacement reactions are shown as arrows.

Figure 2a shows that pyrochlore may coexist with lueshite under conditions of relatively high a_{Na^+} during carbonatite formation. Although stable three-phase assemblages have not been reported in this system, several replacement reactions appear to be quite common. Pyrochlore can be replaced by lueshite, suggesting that a_{Na^+} can be maintained at moderate to high levels during the late magmatic to hydrothermal stages of host rock emplacement. Pyrochlore is also known as a replacement product of natroniobite and fersmite, requiring a decrease in the $a_{Na^+}/a_{Ca^{2+}}$ ratio during subsequent magmatic-hydrothermal evolution.

The phase relations depicted in Figure 2b represent a section at moderate $a_{Fe^{2+}}$ through a three-dimensional Na^+-Ca^{2+}-Fe^{2+} activity diagram (analogous to Figure 2 of Lumpkin and Ewing, 1992). Figure 2b shows that ferrocolumbite can coexist with pyrochlore or fersmite under conditions of moderate $a_{Fe^{2+}}$, moderate $a_{Ca^{2+}}$, and low to moderate a_{Na^+}. Stable three-phase assemblages have not been documented; however, ferrocolumbite is known to replace pyrochlore and fersmite or vice versa, consistent with variable activity ratios during the evolution of the carbonatite magma-fluid system.

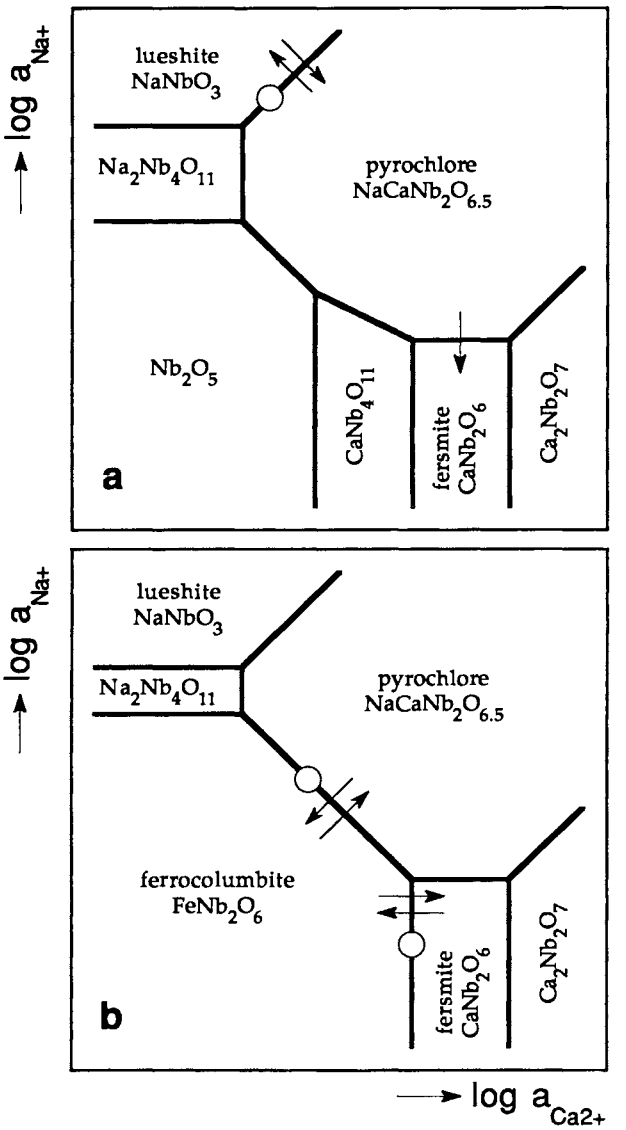

Fig. 2. Qualitative activity diagrams for the system Na-Ca-Fe-Nb-O-H derived from known mineral parageneses. (a) Na-Ca relations at low Fe^{2+} activity. (b) Na-Ca relations at moderate Fe^{2+} activity. Diagrams based on data in Table 2 and Fig. 2 of Lumpkin and Ewing (1992). Circles represent coexisting phases, arrows denote replacement reactions.

Chemical effects of alteration

Experimental procedures used in this investigation are identical to those described by Lumpkin and Ewing (1992) and need not be repeated here. Electron microprobe analyses and structural formulas normalized to 2.000 B-site

TABLE 2. Representative electron microprobe analyses of unaltered and altered areas of six pyrochlore samples

	181	181p	181t	187	187p	187t	325	325p	214	214s	299A	299Bs
Nb_2O_5	60.8	60.9	54.9	60.6	61.8	55.1	47.8	43.9	34.5	35.0	68.0	75.0
Ta_2O_5	0.00	0.00	0.06	0.06	0.05	0.32	10.5	10.1	9.05	8.99	0.03	0.14
TiO_2	3.71	3.90	5.07	3.63	3.90	5.09	0.54	0.44	12.3	11.1	3.18	4.40
ZrO_2	2.69	1.64	2.52	3.24	2.62	2.69	1.35	1.36	0.00	0.00	0.01	0.34
ThO_2	1.45	1.69	4.09	1.08	1.70	3.77	1.49	1.24	1.13	0.89	0.07	0.16
UO_2	0.00	0.00	0.05	0.10	0.13	0.11	22.1	21.6	19.7	18.2	0.00	0.42
Al_2O_3	0.00	0.00	0.02	0.00	0.01	0.02	0.08	0.16	0.07	0.45	0.01	0.16
Y_2O_3	0.25	0.26	0.42	0.24	0.22	0.39	0.00	0.00	0.32	0.94	0.15	0.19
Ln_2O_3	4.5	6.2	9.9	3.3	3.8	7.6	0.08	0.22	0.49	1.3	0.47	0.26
MgO	0.05	0.03	0.11	0.01	0.00	0.07	0.29	0.62	0.07	0.17	0.00	0.00
CaO	17.2	10.4	10.5	16.7	12.6	10.5	8.43	6.60	12.3	6.96	15.3	0.37
MnO	0.04	0.23	0.13	0.09	0.37	0.22	0.00	0.81	0.32	0.22	0.02	0.00
FeO	0.93	2.46	4.00	1.14	2.43	4.55	1.15	0.26	1.91	2.48	0.01	0.54
SrO	0.17	1.41	0.18	0.34	0.73	0.28	0.00	3.97	0.17	0.62	0.67	4.03
BaO	0.04	0.64	0.16	0.00	0.09	0.00	0.02	1.37	0.17	0.40	0.05	1.08
PbO	0.27	0.31	0.23	0.24	0.27	0.15	0.35	0.00	1.76	0.81	0.16	0.18
Na_2O	5.12	3.32	0.22	5.22	4.39	0.23	1.57	0.64	2.14	0.01	7.73	0.00
K_2O	0.00	0.00	0.00	0.00	0.04	0.04	0.04	0.12	0.05	0.07	0.01	1.15
F	3.3	2.3	0.36	3.8	3.3	0.00	1.2	1.4	1.5	0.25	5.4	0.11
Sum	100.52	95.74	92.92	99.79	98.45	91.13	96.99	94.81	97.95	88.86	101.27	88.53
O≡F	−1.39	−0.97	−0.15	−1.60	−1.39	−0.00	−0.50	−0.59	−0.63	−0.11	−2.27	−0.05
Total	99.13	94.77	92.77	98.19	97.06	91.13	96.49	94.22	97.32	88.75	99.00	88.48
	Structural formulas based on Σ B = 2.00											
Nb	1.740	1.761	1.660	1.727	1.736	1.652	1.686	1.672	1.139	1.165	1.854	1.803
Ta	0.000	0.000	0.001	0.001	0.001	0.006	0.223	0.229	0.180	0.180	0.001	0.002
Ti	0.177	0.188	0.255	0.172	0.182	0.254	0.032	0.028	0.676	0.615	0.144	0.177
Zr	0.083	0.051	0.082	0.100	0.080	0.087	0.052	0.055	0.000	0.000	0.000	0.000
Al	0.000	0.000	0.002	0.000	0.001	0.002	0.007	0.016	0.006	0.039	0.001	0.010
Th	0.021	0.025	0.062	0.016	0.024	0.057	0.026	0.024	0.019	0.015	0.001	0.002
U	0.000	0.001	0.001	0.001	0.002	0.002	0.384	0.406	0.320	0.299	0.000	0.005
Y	0.008	0.009	0.015	0.008	0.007	0.014	0.000	0.000	0.012	0.037	0.005	0.005
Ln	0.104	0.145	0.241	0.077	0.086	0.185	0.002	0.007	0.013	0.034	0.010	0.005
Mg	0.005	0.003	0.011	0.001	0.000	0.007	0.034	0.078	0.008	0.019	0.000	0.000
Ca	1.167	0.713	0.753	1.128	0.839	0.746	0.705	0.596	0.962	0.549	0.989	0.021
Mn	0.002	0.012	0.007	0.005	0.020	0.012	0.000	0.058	0.020	0.014	0.001	0.000
Fe	0.049	0.132	0.224	0.060	0.126	0.253	0.075	0.018	0.117	0.153	0.001	0.024
Sr	0.006	0.052	0.007	0.012	0.026	0.011	0.000	0.193	0.007	0.026	0.023	0.124
Ba	0.001	0.016	0.004	0.000	0.002	0.000	0.001	0.045	0.005	0.012	0.001	0.023
Pb	0.005	0.005	0.004	0.004	0.005	0.003	0.007	0.000	0.035	0.016	0.003	0.003
Na	0.629	0.412	0.029	0.638	0.529	0.030	0.238	0.104	0.303	0.001	0.904	0.000
K	0.000	0.000	0.000	0.000	0.003	0.003	0.004	0.013	0.005	0.007	0.001	0.078
Σ A	1.977	1.524	1.358	1.951	1.670	1.321	1.477	1.542	1.825	1.181	1.939	0.290
O	6.304	6.065	6.326	6.172	6.025	6.290	6.569	6.671	6.502	6.150	5.907	5.151
F	0.651	0.472	0.076	0.766	0.639	0.000	0.299	0.378	0.356	0.058	1.031	0.019
Σ (X + Y)	6.955	6.537	6.402	6.938	6.664	6.290	6.868	7.049	6.858	6.208	6.938	5.170

Note: a lower-case letter at the end of the sample number indicates the type of alteration: p = primary alteration, t = transitional alteration, s = secondary alteration. B-site cations are Nb, Ta, Ti, Zr, and Al. All Fe assumed to be Fe^{2+} and allocated to the A-site. Si, Sb, Sn, Cs, W, and Bi are typically near or below detection limits and are not reported. Ln = lanthanide.

cations for unaltered and altered areas of each sample are given in Tables 2 and 3.[1] Eighteen individual oxides plus the sum of nine lanthanide oxides (Ln_2O_3 = La, Ce, Pr, Nd, Sm, Gd, Dy, Er, Yb) are listed together with F for each analysis; the oxides of W, Si, Sn, Sb, Bi, and Cs are typically below detection limits in this group of samples and are not reported. The degree of hydration has been estimated by the difference from 100% for each analysis and has a precision of approximately ±2 wt% H_2O. The validity of these estimates has been confirmed by thermogravimetric analysis and infrared spectroscopy for selected samples (Lumpkin, 1989).

[1] Table 3 may be ordered as Document AM-95-590 from the Business Office, Mineralogical Society of America, 1130 Seventeenth Street NW, Suite 330, Washington, DC 20036, U.S.A. Please remit $5.00 in advance for the microfiche.

Primary alteration

Primary alteration was observed in two uranpyrochlore samples. In sample 325, from the Jacupiranga carbonatite, alteration is characterized by exchange of Ca, Na, and F for Sr, O, and minor Mn, Fe, and Ba. Small amounts of Al, REEs, Mg, Pb, and K were also detected by electron microprobe analysis. Of these elements, REEs increased and Pb decreased as a result of alteration. Structural formulas of unaltered and altered material indicate that only minor changes in the number of A-site and Y-site vacancies occurred during alteration. Specimen 216 is from the MacDonald pegmatite, Hybla, Ontario, Canada. Structural formulas of unaltered and altered areas indicate major increases in Ca and O plus minor increases in Sr coupled with decreased Na, $^{A}\square$, and $^{Y}\square$ (where □ indicates a vacancy). On average, the amount of F decreased only

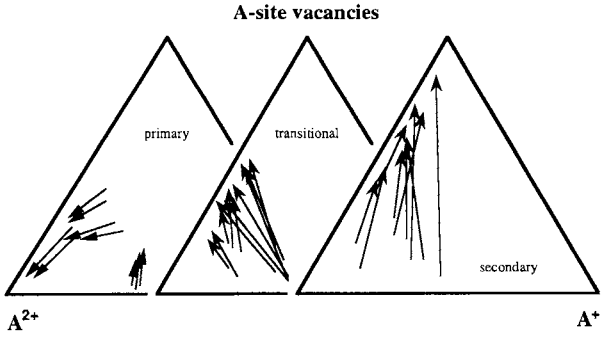

Fig. 3. Triangular plots (atomic percent) of divalent A-site cations (mainly Ca plus some Fe, Sr, and Ba), monovalent A-site cations (mainly Na plus minor K), and A-site vacancies in unaltered and altered pyrochlore samples. Alteration vectors are shown as arrows pointing toward the altered composition.

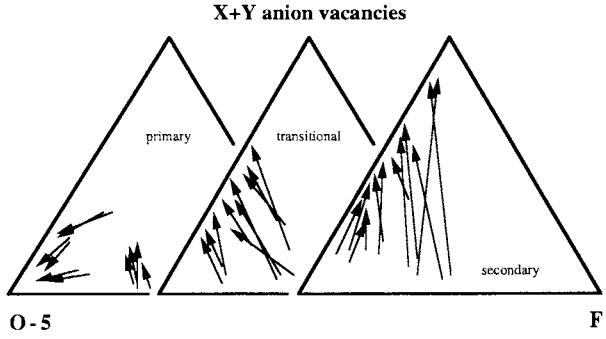

Fig. 4. Triangular plots (atomic percent) of X-site and Y-site anions and X + Y anion vacancies in unaltered and altered pyrochlore samples. The O content is plotted as O − 5 to give the same scale as Fig. 3.

slightly, which suggests that increased O contents were compensated in part by loss of OH groups at the Y site.

Pyrochlore from carbonatites and nepheline syenites exhibits an alteration pattern that differs from the examples described above mainly in the role of vacancies. Structural formulas of specimens 181 and 187 indicate loss of Ca, Na, and F coupled with increased Mn, Fe, Sr, and both A-site and Y-site vacancies. There are also minor to moderate increases in the inferred amount of H_2O in the altered areas of both specimens. The overall alteration pattern resembles secondary alteration observed in members of the microlite subgroup (Lumpkin and Ewing, 1992). It is clear, however, that alteration of these pyrochlores proceeded to a limited extent in terms of the actual number of cations lost (0.3–0.5 A-site cations per formula unit).

Primary alteration patterns are shown graphically in Figures 3–5. In Figure 3, the altered compositions plot toward the A^{2+}- or A-site vacancy corner. Similar trends are shown for the anions in Figure 4, where the altered compositions plot closer to the O − 5 or X + Y anion vacancy corner. The U and Th contents tend to remain relatively constant in most specimens (Fig. 5). Formal substitution schemes compatible with these trends are $^{A}\square^{Y}\square \rightarrow {}^{A}Ca^{Y}O$, $^{A}Na^{Y}F \rightarrow {}^{A}Ca^{Y}O$, $^{A}Na^{Y}F \rightarrow {}^{A}\square^{Y}\square$, and $^{A}Ca^{Y}O \rightarrow {}^{A}\square^{Y}\square$. [For all substitutions the format is unaltered → altered, where the arrow indicates "replaced by" or "goes to." The equivalent exchange operator notation after Burt (1989) is altered(unaltered)$_{-1}$.] Incorporation of Sr during primary alteration of uranpyrochlore from Jacupiranga is consistent with a substitution of the form $^{A}Na^{Y}F \rightarrow {}^{A}Sr^{Y}O$. The substitution $^{A}Na^{Y}OH \rightarrow {}^{A}Ca^{Y}O$ can be inferred in cases where there are only minor changes in the F content. There is little evidence for the simple substitution $^{Y}F \rightarrow {}^{Y}OH$, although at low levels this substitution may be obscured by the chemical complexity of the system.

Of the minor elements, Mn, Fe, and REEs are commonly present in unaltered pyrochlore and may increase, remain relatively constant, or, less commonly, decrease as a result of alteration. The large cations Sr, Ba, and K generally occur at low levels in unaltered material and serve as better chemical indicators of alteration. Figure 6 shows that peak levels of approximately 0.2 Sr, 0.05 Ba, and 0.02 K atoms per formula unit occur at A-site vacancy levels of 0.2–0.6 per formula unit as a result of primary alteration.

A number of chemical reactions may be postulated to account for the primary alteration patterns observed in pyrochlore from granitic pegmatites, nepheline syenites, and carbonatites:

$$H_2O + Ca^{2+} + (CaNb_2O_6)_{pss} = (Ca_2Nb_2O_7)_{pss} + 2H^+ \quad (1)$$

$$H_2O + Ca^{2+} + (NaCaNb_2O_6F)_{pss} = (Ca_2Nb_2O_7)_{pss} + Na^+ + HF + H^+ \quad (2a)$$

$$Ca^{2+} + (NaCaNb_2O_6OH)_{pss} = (Ca_2Nb_2O_7)_{pss} + Na^+ + H^+ \quad (2b)$$

$$0.5H_2O + Ca^{2+} + (NaCaNb_2O_{6.5})_{pss} = (Ca_2Nb_2O_7)_{pss} + Na^+ + H^+ \quad (2c)$$

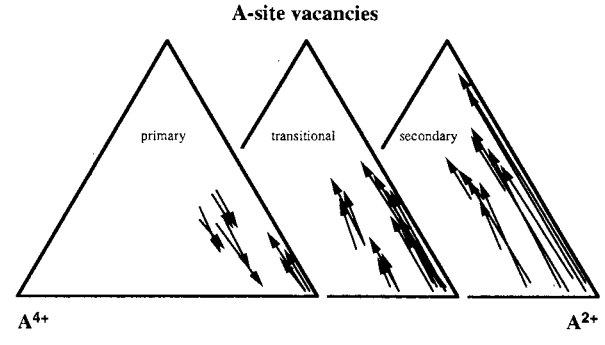

Fig. 5. Triangular plots (atomic percent) of tetravalent A-site cations (Th and U), divalent A-site cations (mainly Ca plus some Fe, Sr, and Ba), and A-site vacancies in unaltered and altered pyrochlore samples.

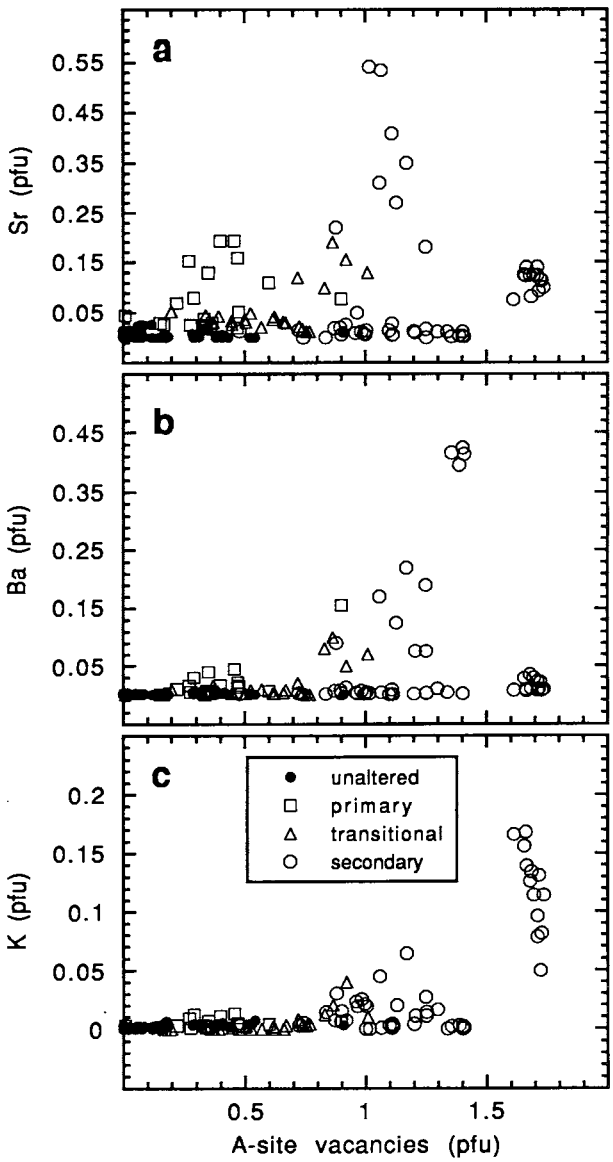

Fig. 6. Plots of large A-site cations (atoms per formula unit) vs. A-site vacancies in unaltered and altered pyrochlores. (a) Sr. (b) Ba. (c) K. Note how each element tends to peak at different vacancy levels as a result of secondary alteration.

$$H_2O + Sr^{2+} + (NaCaNb_2O_6F)_{pss} = (CaSrNb_2O_7)_{pss} + Na^+ + HF + H^+ \quad (3)$$

$$H^+ + (NaCaNb_2O_6F)_{pss} = (CaNb_2O_6)_{pss} + Na^+ + HF \quad (4)$$

$$3H^+ + (NaCaNb_2O_6F)_{pss} = (Nb_2O_5 \cdot H_2O)_{pss} + Na^+ + Ca^{2+} + HF. \quad (5)$$

To account for the presence of F, O, or OH at the Y site, Reaction 2 is given in three forms. Reactions 1–3 suggest that alteration occurs under relatively basic conditions. Reactions 4 and 5 model the alteration observed in samples 181 and 187 and are consistent with relatively acidic conditions during alteration. Estimated increases of 2–5 wt% H_2O (0.4–1.0 molecules per formula unit) are typical for most specimens.

Transitional alteration

Sample 187, from the carbonatite of Alnö, Sweden, provides a good example of transitional alteration observed in members of the pyrochlore subgroup. In comparison with unaltered material, structural formulas of altered areas indicate major loss of Na and F, loss of some Ca, and major increases in REEs and Fe. Hydration, coupled with increasing of A-site and Y-site vacancies, also occurred. This pattern of alteration is identical to that observed in sample 181 from a nepheline syenite host rock in the Langesundfiord district of southern Norway. A similar style of alteration was observed in uranpyrochlore from granitic pegmatites in the Bancroft district, Ontario, Canada (e.g., samples 090 and 289), but minor changes in REEs and Fe were detected in these samples.

As shown in Figures 3 and 4, altered compositions generally involve an increase in A-site vacancies and X + Y anion vacancies at the expense of A^+ cations (mainly Na) and F, which is consistent with a substitution of the form $^{A}Na^{Y}F \rightarrow {}^{A}\square^{Y}\square$. Some Ca loss occurs but is normally compensated in part by cation exchange for Sr, Ba, and REEs. The relative amounts of U and Th remain approximately constant (Fig. 5). Overall transitional alteration produced maximum amounts of approximately 0.2 Sr, 0.08 Ba, and 0.04 K atoms per formula unit at A-site vacancy levels of 0.7–1.1 per formula unit (Fig. 6).

The major chemical changes associated with the transitional alteration of pyrochlore are summarized in Reactions 6–9. Although these reactions are similar to Reaction 4, they include structural H_2O in the alteration product to account for moderate to major increases in the degree of hydration:

$$H^+ + H_2O + (NaCaNb_2O_6F)_{pss} = (CaNb_2O_6 \cdot H_2O)_{pss} + Na^+ + HF \quad (6)$$

$$H^+ + H_2O + Sr^{2+} + (NaCaNb_2O_6F)_{pss} = (SrNb_2O_6 \cdot H_2O)_{pss} + Na^+ + Ca^{2+} + HF \quad (7)$$

$$1.5H_2O + Ce^{3+} + (NaCaNb_2O_6F)_{pss} = (CeNb_2O_{6.5} \cdot H_2O)_{pss} + Na^+ + Ca^{2+} + HF \quad (8)$$

$$H^+ + H_2O + Ba^{2+} + (NaCaNb_2O_6F)_{pss} = (BaNb_2O_6 \cdot H_2O)_{pss} + Na^+ + Ca^{2+} + HF. \quad (9)$$

The salient feature of transitional alteration is loss of Na and F combined with some cation exchange for Sr, Ba, REEs, and Fe to produce a hydrated pyrochlore near $AB_2O_6 \cdot H_2O$ in stoichiometry. H_2O contents estimated from analytical totals suggest that increases of 4–12 wt%

H_2O (0.8–2.4 molecules per formula unit) occurred during this stage of alteration.

Secondary alteration

Chemical changes accompanying alteration are exemplified by sample 084 from Brevik, Norway. Unaltered areas of the sample contain major amounts of Ca, Na, and F. In contrast, altered areas are characterized by reduced Ca, near complete loss of Na and F, increased amounts of Mn, Fe, and REEs, and major increase in the inferred amount of H_2O. The corresponding structural formulas also indicate major increases in $^{A}\square$ and $^{Y}\square$. This style of late, fracture-controlled alteration can be found in pyrochlores from all three of the major host rock categories, commonly cutting across earlier primary or transitional alteration.

Major cation exchange effects are normally limited to pyrochlores found in lateritic environments. Excellent examples include bariopyrochlore 1C24 from Araxá, Minas Gerais, Brazil, and kalipyrochlore 086 and strontiopyrochlore samples 294 and 299B from Lueshe, Lake Kivu, Zaire. The structure formulas of these samples exhibit extreme numbers of A-site, Y-site, and X-site vacancies characteristic of secondary alteration. Effects of secondary alteration on members of the pyrochlore subgroup are summarized in Figures 3–5. Altered compositions plot significantly toward the A-site vacancy corner of Figure 3 and the X + Y anion vacancy corner of Figure 4. The relative amounts of U and Th in these samples remain essentially unchanged (Fig. 5). Maximum numbers of vacancies are 1.7 $^{A}\square$, 1.0 $^{Y}\square$, and 0.8 $^{X}\square$ per formula unit. As shown in Figure 6, maximum amounts of 0.55 Sr, 0.45 Ba, and 0.18 K atoms per formula unit occur at A-site vacancy levels of 0.9–1.7 per formula unit.

Secondary alteration trends are consistent with the substitution schemes $^{A}Ca^{Y}O \rightarrow {}^{A}\square^{Y}\square$, $^{A}Na^{Y}F \rightarrow {}^{A}\square^{Y}\square$, and $^{A}Ca^{X}O \rightarrow {}^{A}\square^{X}\square$. In consideration of cation exchange for Sr, Ba, and K, the alteration process can be approximated by reactions of the form:

$$3H^+ + H_2O + (NaCaNb_2O_6F)_{pss} = (Nb_2O_5 \cdot 2H_2O)_{pss} + Na^+ + Ca^{2+} + HF \quad (10)$$

$$2H^+ + 1.5H_2O + 0.5Ba^{2+} + (NaCaNb_2O_6F)_{pss} = (Ba_{0.5}Nb_2O_{5.5} \cdot 2H_2O)_{pss} + Na^+ + Ca^{2+} + HF \quad (11)$$

$$2H^+ + 1.5H_2O + 0.5Sr^{2+} + (NaCaNb_2O_6F)_{pss} = (Sr_{0.5}Nb_2O_{5.5} \cdot 2H_2O)_{pss} + Na^+ + Ca^{2+} + HF \quad (12)$$

$$2H^+ + 1.5H_2O + K^+ + (NaCaNb_2O_6F)_{pss} = (KNb_2O_{5.5} \cdot 2H_2O)_{pss} + Na^+ + Ca^{2+} + HF. \quad (13)$$

Reactions 11–13 require a source of Ba, Sr, and K. In carbonatites, these elements are normally supplied by the dissolution of feldspars and carbonate minerals during laterite formation. Breakdown of carbonate minerals (i.e., ankerite, siderite, bastnaesite, etc.) may also provide much of the Fe and REEs incorporated by pyrochlore during secondary alteration. Silicate minerals are the likely sources of Ba, Sr, REEs, and other elements incorporated by pyrochlores during late stage alteration of nepheline syenite pegmatites. Reactions 10–13 involve hydration of the pyrochlore phase and should proceed to the right under conditions of low T, pH, a_{Na^+}, a_{HF}, and $a_{Ca^{2+}}$. Estimated increases in H_2O content as a result of secondary alteration range from approximately 8 to 14 wt% (1.5–2.8 molecules per formula unit) for most specimens.

Behavior of REEs

Pyrochlore from carbonatites and nepheline syenites is strongly enriched in the light lanthanides La through Sm, with Ce typically accounting for 65–75% of the total REE content. Lanthanides heavier than Sm were rarely detected above the 0.1 wt% level and Y contents were low, typically 0.0–0.4 wt% Y_2O_3. Uranpyrochlore from granitic pegmatites has lower total lanthanide contents (Ce is commonly the only lanthanide significantly above background) and slightly higher Y contents, typically 0.1–0.6 wt% Y_2O_3. For unaltered pyrochlore, we found Y/Ce atomic ratios of 0.16 ± 0.04 (range 0.10–0.23), 0.27 ± 0.13 (range 0.11–0.56), and 1.4 ± 0.5 (range 0.8–3.5) for samples from nepheline syenites, carbonatites, and granitic pegmatites, respectively. This trend is generally consistent with the results of Fleischer (1965) and Fleischer and Altschuler (1969), suggesting that Y/Ce ratios or chondrite-normalized abundance patterns of unaltered and altered areas of pyrochlore might reflect relative changes in pH (Burt and London, 1982; Burt, 1989).

Even though the total REEs in pyrochlore may increase in abundance by as much as a factor of two as a result of alteration, data shown in Figure 7 suggest that chondrite-normalized abundance patterns do not change significantly. Unfortunately, REEs heavier than Gd are near or below detection limits in the samples analyzed in this study, thus limiting the usefulness of abundance patterns. The observed Y/Ce ratios of most of the pyrochlores analyzed in this study did not change significantly as a result of primary or transitional alteration. However, secondary alteration commonly resulted in an increase in the Y/Ce ratio. As a result of alteration, the Y/Ce ratio of samples 298, 214, and 299A,B increased from 0.14 to 0.23, 1.2 to 2.1, and 0.5 to 2.0, respectively. These results are consistent with the relatively lower values of pH predicted by Reactions 10–13.

U-Pb systematics

Uranpyrochlore from 1000 m.y. old Grenville rocks in the Bancroft area, Ontario, Canada, typically contain 17–28 wt% UO_2 and <1.0 wt% ThO_2 and are completely metamict. The U and Pb contents plotted in Figure 8 indicate Pb loss of up to 80–85% in both altered and unaltered material, consistent with a model of long-term Pb loss. However, there is a tendency for unaltered samples to fall closer to the 1000 m.y. reference line. Three

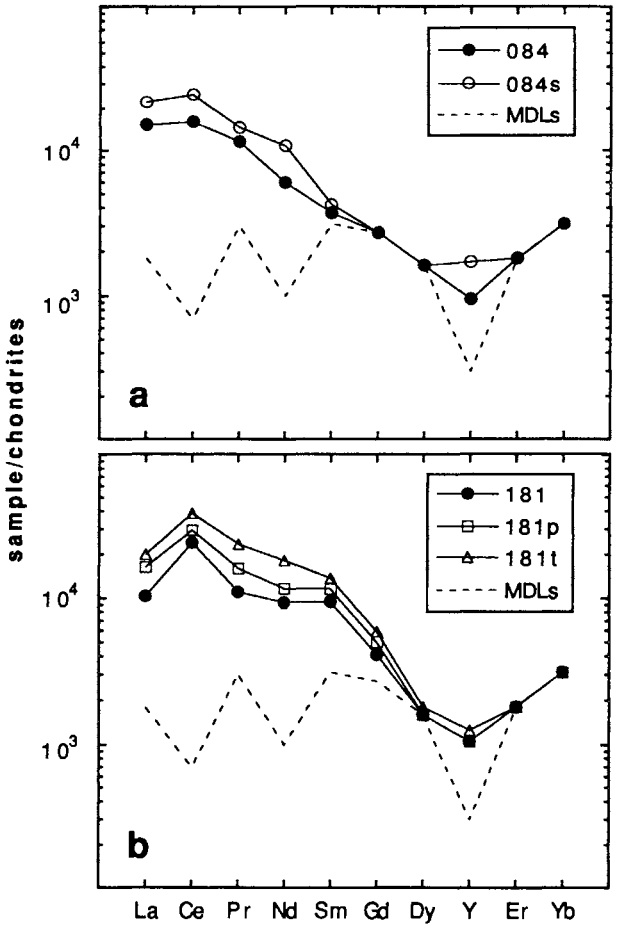

Fig. 7. Chondrite-normalized REE distribution patterns of unaltered and altered pyrochlores. (a) Sample 084. (b) Sample 181. Letters at the end of the sample number refer to the type of alteration: p = primary, t = transitional, and s = secondary. MDLs = minimum detection limits.

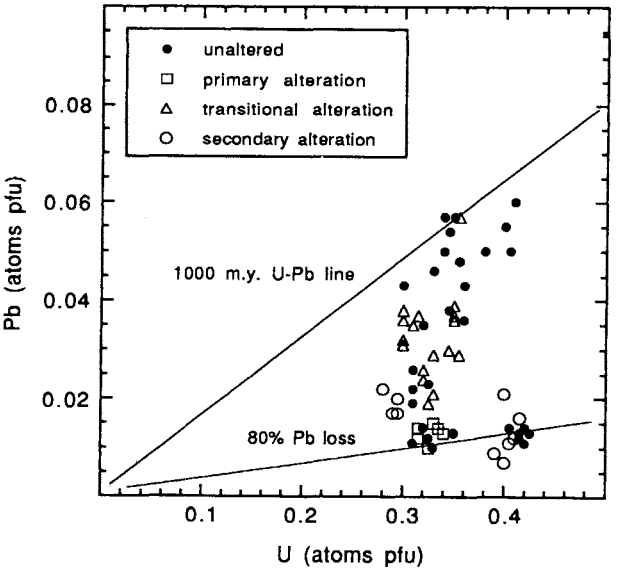

Fig. 8. U-Pb systematics of unaltered and altered areas of uranpyrochlore samples from approximately 1000 m.y. old Grenville rocks, eastern Canada. In these samples, the altered areas tend to plot further below the 1000 m.y. U-Pb line.

samples in particular show Pb loss associated with alteration. Assuming all Pb to be radiogenic, unaltered areas of sample 289 give an average U-Pb age of 1005 ± 65 m.y. In contrast, altered areas of the sample give an average age of 560 ± 115 m.y., indicating 40% Pb loss during alteration. Average U-Pb ages for sample 090 are 870 ± 55 m.y. for unaltered and 635 ± 85 m.y. for altered areas, consistent with Pb loss of 25% during alteration. Analyses of sample 191 give U-Pb ages of 910 ± 50 m.y. and 100 ± 25 m.y. for unaltered and altered material, respectively. This is the most extreme case encountered, indicating loss of about 90% of the radiogenic Pb during secondary alteration.

Disturbance of U-Pb systematics can also occur in relatively young specimens as indicated by electron microprobe analyses of uranpyrochlore 325 from the carbonatite of Jacupiranga, Brazil. Unaltered cores of several grains give an average U-Pb age of 125 ± 20 m.y., consistent with K-Ar isotopic age determinations of 136 m.y. for whole rock samples of carbonatite and pyroxenite (Amaral et al., 1967) and U-Pb isotopic ages of 127 ± 5 and 132 ± 5 m.y. for two grains of zirconolite from unweathered pyroxenite (Oversby and Ringwood, 1981). Altered rims on the same grains consistently give lower Pb contents, leading to an average U-Pb age of 75 ± 20 m.y. X-ray diffraction data show that the crystals are partially crystalline (see Table 1), but the calculated dose of 7–8 × 10^{16} α/mg is well above the saturation dose of 1 × 10^{16} α/mg and therefore the crystals should be fully metamict (Lumpkin and Ewing, 1988). Subsequent TEM investigation revealed that the unaltered cores are in fact metamict, but the rims exhibit a recrystallized microstructure. These results indicate ~40% Pb loss during primary alteration and recrystallization of the Jacupiranga uranpyrochlore.

Discussion

Chemical effects of alteration

The major chemical changes that accompany alteration are summarized in terms of idealized end-members in Figure 9. Unaltered compositions generally project within the $NaCaNb_2O_6F$-$Ca_2Nb_2O_7$-$CaNb_2O_6$ composition field. Composition vectors in this system correspond to four substitutions: **1** = $^{A}\square^{Y}\square \rightarrow {}^{A}Ca^{Y}O$, **2** = $^{A}Na^{Y}F \rightarrow {}^{A}Ca^{Y}O$, **3** = $^{A}Na^{Y}F \rightarrow {}^{A}\square^{Y}\square$, and **4** = $^{A}Ca^{Y}O \rightarrow {}^{A}\square^{Y}\square = -1$ (above 50 mol% of the defect pyrochlore component, vector **4** = $^{A}Ca^{X}O \rightarrow {}^{A}\square^{X}\square$). Primary alteration paths (P1) of uranpyrochlore from granitic pegmatites and carbonatites tend to fall between vectors **1** and **2**, much like those of the microlite subgroup (Lumpkin and Ewing, 1992). In contrast, primary alteration paths (P2) of pyro-

chlore from nepheline syenites and carbonatites fall between vectors **3** and **4**. Transitional alteration paths (T) scatter in a broad area between vectors **2** and **4**, generally falling between the alteration paths observed for primary and secondary alteration (S).

With progressive primary and transitional alteration, minerals of the pyrochlore subgroup exhibit A-site cation exchange for Sr, Fe, and Mn relatively early. During the later stages of alteration, Sr and Mn tend to decrease, whereas Fe continues to increase along with Ba and REEs. Significant changes in the REE abundance patterns or Y/Ce ratios of pyrochlore were not observed for primary or transitional alteration, indicating that actual pH changes were minor and that alteration was largely controlled by variations in the activities of cations, HF, and H_2O. Moderate to major increases in K, Sr, and Ba are typical of secondary alteration in tropical climates (Jäger et al., 1959; Harris, 1965; Van Wambeke, 1978). As a result of secondary alteration, a few samples exhibit changes in Y/Ce ratio that are qualitatively consistent with relatively low values of pH inferred from exchange reactions. However, the use of REEs to monitor pH during alteration of pyrochlore requires caution because of crystal chemical factors (Fleischer, 1965; Burt, 1989; Mariano, 1989).

Although recent evidence indicates that high valence cations like Ti and Zr (along with REEs, Th, and U) are mobile under hydrothermal conditions (Gieré, 1986, 1990; Williams and Gieré, 1988; Gieré and Williams, 1992; Flohr, 1994), the major B-site cations Nb, Ta, Ti, and Zr are relatively immobile once incorporated into the stable framework structure of pyrochlore. Although the results of this investigation also show that Th and U are immobilized quite effectively by pyrochlore, the behavior of radiogenic Pb is variable. Analyses of unaltered uranpyrochlore suggest that up to 80% of the radiogenic Pb may have been lost by long-term diffusion and removal from the radiation damaged samples by fluids migrating along cracks and microfractures (Lumpkin and Ewing, 1992). In many of these samples there is also evidence for episodic loss of 25–90% of the radiogenic Pb as a result of primary, transitional, or especially secondary alteration.

Most of the results described above are related to the remarkable ability of the pyrochlore structure to tolerate vacancies at the A, X, and Y sites stabilized by the incorporation of H_2O molecules and OH groups (up to 10–15 wt% total H_2O). Both the A and Y sites are located within channels parallel to {110} formed by the stable B_2X_6 framework of pyrochlore. Cation-anion pairs (e.g., Na-F, Ca-O) located on these sites can be removed from the structure in response to chemical potential gradients, resulting in paired vacancies (Schottky defects). Additional Schottky defects are produced by limited removal of Ca-O pairs from the A and X sites. Loss of anions can be partially offset by exchange for large monovalent and divalent cations like K, Sr, and Ba. Ionic conduction by charge-balanced A-Y and A-X pairs provides a first order constraint on the cation exchange capacity of pyrochlore

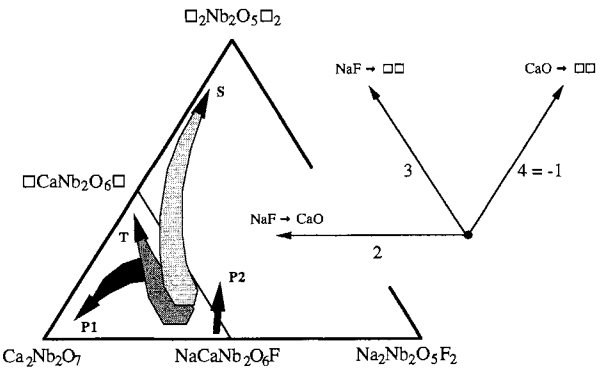

Fig. 9. Composition vectors and triangular plot of pyrochlore end-members summarizing observed geochemical alteration patterns. P1 = primary alteration of uranpyrochlore from granitic pegmatites, P2 = primary alteration of sodium calcium pyrochlore from nepheline syenites and carbonatites, T = transitional alteration, and S = secondary alteration.

on the basis of the formal valence of the A-site cation: $A^+ > A^{2+} \gg A^{3+} \gg A^{4+}$. This sequence, modified by the additional effect of cation size, gives a reasonable explanation for the observed cation mobility sequence in pyrochlore: Na > Ca > Sr > Ba > K > REEs > Th, U.

Conditions of alteration

As summarized previously by Lumpkin and Ewing (1992), members of the microlite subgroup undergo primary alteration during the late magmatic to hydrothermal stages of highly fractionated, complex pegmatites of the spodumene and lepidolite type. The alteration typically occurs at P = 2–4 kbar and T = 350–550 °C in the presence of a Na-K-Al silicate liquid and an exsolved, saline H_2O-CO_2 fluid rich in Li, Be, B, F, P, Mn, Rb, Cs, and Ta. Members of the pyrochlore subgroup (mainly uranpyrochlore) are generally restricted to geochemically more primitive granitic pegmatites of the rare earth, beryl, and beryl-columbite type (Černý, 1989; Černý and Ercit, 1989). These rock types typically have higher Ti, Fe, Nb, and REE contents and lower levels of volatiles, Mn, and Ta than their more highly fractionated counterparts. As a result, the magmatic-hydrothermal conditions characteristic of uranpyrochlore crystallization and subsequent primary alteration may be shifted to higher temperatures toward the granite solidus, giving an approximate temperature range of 450–650 °C at 2–5 kbar (see Černý, 1989, Fig. 2). Exchange reations between uranpyrochlore and the hydrothermal fluid suggest conditons of relatively high pH, high $a_{Ca^{2+}}$, and low a_{Na^+}, accompanied by elevated $a_{Fe^{2+}}$ and $a_{Sr^{2+}}$ during primary alteration.

In contrast to granitic pegmatites, carbonatites and nepheline syenites are typically emplaced at shallower depths of 0–5 km ($P \approx$ 0–2 kbar) as part of comparatively large, alkaline igneous complexes. Experimental work and field observations suggest that the magmatic phase of carbonatite emplacement may have concluded

at temperatures as low as 450–500 °C, with continued hydrothermal activity to 200–300 °C (Aleksandrov et al., 1975; Heinrich, 1980). The magmatic phase of host rock emplacement is of relatively long duration, and associated hydrothermal activity may continue throughout the period of uplift and erosion, thus accounting for the range of alteration effects observed in minerals of the pyrochlore subgroup. During this time, the hydrothermal fluid may evolve from primarily magmatic fluid at deeper crustal levels to one dominated by ground water near the surface (Andersen, 1984, 1987; Flohr, 1994).

In carbonatites, most of the pyrochlore crystallized in the presence of an alkali-carbonate magma and exsolved fluid rich in CO_2, F, P, Ti, Fe, Sr, Zr, Nb, Ba, REEs, Th, and U after crystallization of diopside, forsterite, phlogopite, and most of the calcite. Primary alteration of pyrochlore probably occurred during subsequent formation of tremolite, dolomite, and ankerite. The subsolidus reactions tremolite + calcite = diopside + forsterite and tremolite + dolomite = forsterite + calcite ($T \approx 450$–550 °C, $X_{CO_2} \approx 0.05$–0.95, $P = 1$ kbar: Rice and Ferry, 1982) provide an estimate of the upper limit of primary alteration. Exchange reactions between pyrochlore and the hydrothermal fluid are generally consistent with relatively low pH, low a_{HF}, low a_{Na^+}, low $a_{Ca^{2+}}$, and elevated activities of Mn, Fe, and Sr during alteration.

The next stage of carbonatite emplacement is characterized by alteration of olivine to serpentine, pyroxene to sodium amphibole, tremolite to talc, and phlogopite to talc or chlorite, together with the formation of bastnaesite, monazite, barite, fluorite, quartz, and sulfides. At low pressure, alteration of tremolite to talc can occur at temperatures below 300–450 °C over a range of X_{CO_2} (~0.0–0.8), but serpentinization of olivine requires a fluid composition with very low values of X_{CO_2} (<0.05) and temperatures below 300–350 °C (Winkler, 1979). Replacement reactions involving pyrochlore, columbite, and fersmite occurred at this time (Heinrich, 1980), indicating that the fluid had relatively high $a_{Fe^{2+}}$ and low a_{Na^+}. Transitional alteration of pyrochlore probably took place during this stage in the presence of a medium- to low-temperature (200–350 °C) hydrothermal fluid with relatively low pH, low a_{HF}, low a_{Na^+}, low $a_{Ca^{2+}}$, high $a_{Sr^{2+}}$, high $a_{Ba^{2+}}$, and high $a_{REE^{3+}}$.

Secondary alteration of pyrochlore mainly occurred at low temperatures (<150 °C) by exposure to ground water with relatively low pH, low concentrations of Na, Ca, and F, and significant amounts of Mg, Al, K, Fe, Sr, Ba, and REEs derived from dissolution of silicate and carbonate minerals. In some carbonatites, especially those exposed to large volumes of ground water in tropical climates, large quantities of altered pyrochlore are concentrated in laterite horizons (e.g., Jäger et al., 1959; Harris, 1965; Van Wambeke, 1971; von Maravić, 1983), demonstrating that the ion exchange rate far exceeds the dissolution rate of pyrochlore under these conditions. The results presented in this study are in accordance with experimental studies, which have shown that defect pyrochlore readily undergoes ion exchange and hydration at temperatures below 500 °C in acid or salt solutions (e.g., Michel et al., 1975; Goodenough et al., 1976; Groult et al., 1982; see Subramanian et al., 1983, for a review).

Conclusions

Members of the pyrochlore subgroup serve as useful indicators of geochemical processes over a broad range of *PTX* conditions involving granitic pegmatites, nepheline syenites, carbonatites, and their evolved hydrothermal fluids. Although the basic alteration mechanisms of cation exchange and leaching are similar to those of the microlite subgroup, many samples of the pyrochlore subgroup exhibit alteration effects that are transitional between the previously identified extremes of primary (hydrothermal) and secondary (near surface) alteration. A better understanding of the conditions of alteration can be obtained only through a combination of experimental work and detailed studies of individual mineral deposits.

With regard to the disposal of nuclear waste using ceramic materials such as Synroc (Ringwood et al., 1988), various tailored ceramics (Harker, 1988), and lanthanum zirconium pyrochlore (Hayakawa and Kamizono, 1993), this study demonstrates that minerals of the pyrochlore subgroup are susceptible to alteration over a considerable range of conditions. However, the alteration mechanisms are subject to charge-balance constraints that limit the mobility of REEs and, in particular, Th and U. Another paper will address the geochemical stability of the betafite subgroup, providing information on U-rich, heavily radiation-damaged samples in which Ti is a major B-site framework cation.

Acknowledgments

This paper is dedicated to the late Doug Brookins and his many accomplishments in the field of geochemistry. We thank Carl Francis (Harvard University), John White (Smithsonian Institution), George Harlow (American Museum of Natural History), and Anthony Mariano for providing many of the pyrochlore samples. The manuscript was improved through reviews by Don Burt and one anonymous referee. Most of the research was completed in the Electron Microbeam Analysis Facility in the Department of Earth and Planetary Sciences at the University of New Mexico, supported in part by NSF, NASA, DOE-BES (grant DE-FG03-93ER45498), and the State of New Mexico.

References cited

Aleksandrov, I.V., Trusikova, T.A., and Tupitsin, B.P. (1975) The geochemistry of niobium and tantalum in the carbonatite process. In A.I. Tugarinov, Ed., Recent contributions to geochemistry and analytical chemistry, p. 335–344. Wiley, New York.

Amaral, G., Bushee, J., Cordani, U.G., Kawashita, K., and Reynolds, J.H. (1967) Potassium-argon ages of alkaline rocks from southern Brazil. Geochimica et Cosmochimica Acta, 31, 117–142.

Anderson, T. (1984) Secondary processes in carbonatites: Petrology of "rødberg" (hematite-calcite-dolomite carbonatite) in the Fen central complex, Telemark (South Norway). Lithos, 17, 227–245.

——(1987) A model for the evolution of hematite carbonatite, based on whole-rock major and trace element data from the Fen complex, southeast Norway. Applied Geochemistry, 2, 163–180.

Burt, D.M. (1989) Compositional and phase relations among rare earth element minerals. In Mineralogical Society of America Reviews in Mineralogy, 21, 259–307.

Burt, D.M., and London, D. (1982) Subsolidus equilibria. In Mineralogical Association of Canada Short Course Handbook, 8, 329–346.

Černý, P. (1989) Characteristics of pegmatite deposits of tantalum. In P. Müller, P. Černý, and F. Saupe, Eds., Lanthanides, tantalum and niobium, p. 195–239. Springer-Verlag, Berlin.

Černý, P., and Ercit, T.S. (1989) Mineralogy of niobium and tantalum: Crystal chemical relationships, paragenetic aspects and their economic implications. In P. Müller, P. Černý, and F. Saupe, Eds., Lanthanides, tantalum and biobium, p. 27–29. Springer-Verlag, Berlin.

Ewing, R.C. (1975) Alteration of metamict, rare-earth, AB_2O_6-type Nb-Ta-Ti oxides. Geochimica et Cosmochimica Acta, 39, 521–530.

Fleischer, M. (1965) Some aspects of the geochemistry of yttrium and the lanthanides. Geochimica et Cosmochimica Acta, 29, 755–772.

Fleischer, M., and Altschuler, Z.S. (1969) The relationship of the rare-earth composition of minerals to geological environment. Geochimica et Cosmochimica Acta, 33, 725–732.

Flohr, M.J.K. (1994) Titanium, vanadium, and niobium mineralization and alkali metasomatism from the Magnet Cove Complex, Arkansas. Economic Geology, 89, 105–130.

Gieré, R. (1986) Zirconolite, allanite and hoegbomite in a marble skarn from the Bergell contact aureole: Implications for mobility of Ti, Zr and REE. Contributions to Mineralogy and Petrology, 93, 459–470.

——— (1990) Hydrothermal mobility of Ti, Zr and REE: Examples from the Bergell and Adamello contact aureoles (Italy). Terra Nova, 2, 60–67.

Gieré, R., and Williams, C.T. (1992) REE-bearing minerals in a Ti-rich vein from the Adamello contact aureole (Italy). Contributions to Mineralogy and Petrology, 112, 83–100.

Goodenough, J.B., Hong, H.Y.-P., and Kafalas, J.A. (1976) Fast Na^+-ion transport in skeleton structures. Materials Research Bulletin, 11, 203–220.

Groult, D., Pannetier, J., and Raveau, B. (1982) Neutron diffraction study of the defect pyrochlores $TaWO_{5.5}$, $HTaWO_6$, $H_2Ta_2O_6$, and $HTaWO_6 \cdot H_2O$. Journal of Solid State Chemistry, 41, 277–285.

Harker, A.B. (1988) Tailored ceramics. In W. Lutze and R.C. Ewing, Eds., Radioactive waste forms for the future, p. 335–392. North-Holland, Amsterdam.

Harris, P.M. (1965) Pandaite from the Mrima niobium deposit (Kenya). Mineralogical Magazine, 35, 277–290.

Hayakawa, I., and Kamizono, H. (1993) Durability of an $La_2Zr_2O_7$ waste form containing various amounts of simulated HLW elements. Journal of Nuclear Materials, 202, 163–168.

Heinrich, E.Wm. (1980) The geology of carbonatites, p. 186–215. Krieger, Huntington, New York.

Hogarth, D.D. (1961) A study of pyrochlore and betafite. Canadian Mineralogist, 6, 610–633.

——— (1977) Classification and nomenclature of the pyrochlore group. American Mineralogist, 62, 403–410.

Jäger, E., Niggli, E., and van der Veen, A.H. (1959) A hydrated barium-strontium pyrochlore in a biotite rock from Panda Hill, Tanganyika. Mineralogical Magazine, 32, 10–25.

James, T.C., and McKie, D. (1958) The alteration of pyrochlore to columbite in carbonatites in Tanganyika. Mineralogical Magazine, 31, 889–900.

Krivokoneva, G.K., and Sidorenko, G.A. (1971) The essence of the metamict transformation in pyrochlores. Geochemistry International, 8, 113–122.

Lumpkin, G.R. (1989) Alpha-decay damage, geochemical alteration, and crystal chemistry of pyrochlore group minerals. Ph.D. dissertation, University of New Mexico, Albuquerque, New Mexico.

Lumpkin, G.R., and Ewing, R.C. (1985) Natural pyrochlores: Analogues for actinide host phases in radioactive waste forms. In C.M. Jantzen, J.A. Stone, and R.C. Ewing, Eds., Scientific basis for nuclear waste management VIII, Materials Research Society Symposium Proceedings, vol. 44, p. 647–654. Materials Research Society, Pittsburgh, Pennsylvania.

——— (1988) Alpha-decay damage in minerals of the pyrochlore group. Physics and Chemistry of Minerals, 17, 2–20.

——— (1992) Geochemical alteration of pyrochlore group minerals: Microlite subgroup. American Mineralogist, 77, 179–188.

Mariano, A.N. (1989) Economic geology of rare earth elements. In Mineralogical Society of America Reviews in Mineralogy, 21, 309–348.

Michel, C., Groult, D., and Raveau, B. (1975) Proprietes d'echange d'ions des pyrochlores AB_2O_6: I. Preparation et etude structurale de nouveaux pyrochlores $AMWO_6 \cdot H_2O$ (A = Li, Na: M = Nb, Ta, Sb). Journal of Inorganic and Nuclear Chemistry, 37, 247–250.

Oversby, V.M., and Ringwood, A.E. (1981) Lead isotopic studies of zirconolite and perovskite and their implications for long range SYNROC stability. Radioactive Waste Management, 1, 289–308.

Perrault, G. (1968) La composition chimique et la structure cristalline du pyrochlore d'Oka, P.Q. Canadian Mineralogist, 9, 383–402.

Petruk, W., and Owens, D.R. (1975) Electron microprobe analyses for pyrochlores from Oka, Quebec. Canadian Mineralogist, 13, 282–285.

Rice, J.M., and Ferry, J.M. (1982) Buffering, infiltration, and the control of intensive variables during metamorphism. In Mineralogical Society of America Reviews in Mineralogy, 10, 263–326.

Ringwood, A.E., Kesson, S.E., Reeve, K.D., Levins, D.M., and Ramm, E.J. (1988) Synroc. In W. Lutze and R.C. Ewing, Eds., Radioactive waste forms for the future, p. 233–334. North-Holland, Amsterdam.

Skorobogatova, N.V. (1963) A variety of rare earth pyrochlore from albitites. In A.I. Ginzberg, Ed., New data on rare element mineralogy, p. 108–114. Consultants Bureau, New York.

Subramanian, M.A., Aravamudan, G., and Subba Rao, G.V. (1983) Oxide pyrochlores—A review. Progress in Solid State Chemistry, 15, 55–143.

van der Veen, A.H. (1960) The alteration of pyrochlore to fersmite in the Mbeya carbonatite. Geologie en Mijnbouw, 39, 512–515.

——— (1963) A study of pyrochlore. Verhandelingen van het Koninklijk Nederlands geologisch mijnbouwkundig genootschap, Geologische serie, 22, 1–188.

Van Wambeke, L. (1970) The alteration process of the complex titano-niobo-tantalates and their consequences. Neues Jahrbuch für Mineralogie Abhandlungen, 112, 117–149.

——— (1971) Pandaite, baddeleyite and associated minerals from the Bingo niobium deposit, Kivu, Democratic Republic of Congo. Mineralium Deposita, 6, 153–155.

——— (1978) Kalipyrochlore, a new mineral of the pyrochlore group. American Mineralogist, 63, 528–530.

von Maravić, H.C.R. (1983) Geochemische und petrographische untersuchungen zur genese des niobführenden karbonatit/cancrinit-syenit-komplexes von Lueshe, Kivu/NE-Zaire. Ph.D. dissertation, Technischen Universität, Berlin.

Williams, C.T., and Gieré, R. (1988) Metasomatic zonation of REE in zirconolite from a marble skarn at the Bergell contact aureole (Switzerland/Italy). Schweizerische Mineralogische und Petrographische Mitteilungen, 68, 133–140.

Winkler, H.G.F. (1979) Petrogenesis of metamorphic rocks (5th edition), 348 p. Springer-Verlag, New York.

Manuscript received September 22, 1994
Manuscript accepted March 18, 1995